JOURNAL OF CATALYSIS 115, 194–204 (1989)

NMR Studies of ^{65}Cu and ^{133}Cs in Alkali-Metal-Promoted Copper Catalysts

PO-JEN CHU,* B. C. GERSTEIN,* G. R. SHEFFER,† AND T. S. KING†,[1]

*Departments of *Chemistry and †Chemical Engineering, Ames Laboratory,[2] Iowa State University, Ames, Iowa 50011*

Received June 8, 1988; revised August 25, 1988

A series of unsupported alkali-promoted (Li, Na, K, Rb, Cs) copper catalysts that were found to be active and selective for the conversion of syngas to methanol were investigated by NMR of ^{65}Cu and ^{133}Cs. NMR of ^{65}Cu in the catalysts and in several model compounds, Cu_2O, CuLiO, CuCl, and the like, indicated a "Cu^+-like" species to be present in the catalysts. An identification of compounds in the catalysts was made through NMR of ^{133}Cs in the Cs-promoted catalysts and in several cesium salts. It is inferred from the present work that (i) approximately 10% of the total copper is in the form of $Cs_xCu_{(1-x)}CO_3$ in the mixed carbonate (most of cesium appears as cesium carbonate) and (ii) the catalytic activity for methanol production correlates with the Cu^+ content for different alkali. This correlation leads to the conclusion that Cu^+ is the active center in the syngas conversion. These observations are consistent with the fact that the lithium-promoted catalyst is the least active because the Cu^+ phase is stabilized poorly in the mixed Li–Cu carbonate structure.

INTRODUCTION

Alkali–metal-promoted copper has recently been found to be an active catalyst for methanol synthesis (1, 2). Simple chemical analysis of X-ray structure analyses are not always effective means of identifying oxidation states of transition metals or equilibrium phases present in such materials for several reasons, one being that the catalysts may be nonstoichiometric with the possibility of metal–metal bonding present and another being that the active phase may be present only in localized structures too small for coherent X-ray scattering. Nuclear magnetic resonance offers a possibility of probing oxidation states and possible local environments of atoms in such systems, via interferences from relaxation times and from comparisons of chemical shifts with known compounds.

The present study was initiated in an attempt to identify the active agent in these catalysts, utilizing solid-state nuclear magnetic resonance of the NMR active nuclei ^{133}Cs and ^{65}Cu. The use of NMR for probing heterogeneous catalysts has been recently reviewed (*3*). The various interactions to which nuclei in solids are sensitive make solid-state NMR a powerful tool for such studies (*4*).

Properties of the magnetic isotopes investigated in this study are given in Table 1 (*5*). Note that the 2+ oxidation state of copper can be paramagnetic, resulting in rapid longitudinal relaxation and, consequently, the inability to observe it in our spectrometer. Also, note that the large quadrupole moments of the Cu nuclei yield quadrupolar coupling constants, e^2qQ, of the order of 50 MHz in normal electric field gradients (EFG) and that they produce a central $(\frac{1}{2},-\frac{1}{2})$ transition of the order of a few hundred kilohertz for this spin $\frac{3}{2}$ species (*5–7*). The resulting powder lineshapes obtained by utilizing pulse NMR are, therefore, subject to the distortions due to the flip angle variations across a spectral width large com-

[1] To whom correspondence should be addressed.

[2] Operated for the U.S. Department of Energy by Iowa State University under Contract W-7405-Eng-82. This research was supported by the Assistant Secretary for Energy Research, Office of Energy, Sciences, WPAS-KC-03-02-01.

0021-9517/89 $3.00

TABLE 1

Properties of the Magnetic Isotopes Studied in this Work[a]

Nucleus	I	Abundance (%)	Absolute sensitivity	Q^b	Y^c	ν_0(MHz)
^{63}Cu	$\frac{3}{2}$	69.1	6.43×10^{-2}	−0.16	1.1284	58.53
^{65}Cu	$\frac{3}{2}$	30.9	3.52×10^{-2}	−0.15	1.2089	62.65
^{133}Cs	$\frac{7}{2}$	100.0	4.74×10^{-2}	−0.003	0.5585	28.97

[a] From Ref. (*4*).
[b] Quadrupole moment in 10^{-28} m^2.
[c] Gyromagnetic ratio in kHz/G.

pared to that of the pulse used and also to distortions due to the evolution of the large internal Hamiltonian during the radiofrequency (rf) pulse.

In addition, the existence of conduction electrons in these systems creates broadening associated with the Knight shift (*8*). The anisotropy of this interaction, which is proportional to the magnetic susceptibility anisotropy, can be as large as a few percent with resulting linewidths of 1–2 MHz.

Because of the relative insensitivity of the copper nucleus to detection by NMR and the broadening mechanisms mentioned above, previous NMR studies of copper measurements have been limited to copper nuclei with high local symmetry where the electric field gradient is minimized (*9, 10*) or to the quadrupole regime where the Zeeman interaction is a perturbation on the quadrupole interaction (*5, 6, 11*). To study the wide-line Cu NMR spectra the present study utilizes fast signal digitization, an optimized probe quality factor versus rf power, and a large number of scans to reduce the above-mentioned artifacts. It is the intent of the present work to correlate catalytic activity of the materials under study with the presence and identities of phases containing copper.

The other nucleus in the current study, ^{133}Cs, has a natural abundance of 100%, a nuclear spin $I = \frac{7}{2}$, and a relatively weak quadrupole moment of $-3.0 \times 10^{-3}/10^{-28}$ m^2 (*4, 12*). The relatively low gyromagnetic ratio and the low molar content of Cs in the samples make this nucleus difficult to observe. Under normal electric field gradients, the quadrupole coupling constant for cesium is in the range of a few hundred kilohertz (*13*). The central transition of cesium under a weak quadrupole interaction is governed mainly by the shift anisotropy since the first as well as higher order quadrupolar perturbations can be neglected. Because of both the high spin and the relatively low quadrupolar coupling constant, the first satellite transitions, $(\frac{3}{2}, \frac{1}{2})$ and $(-\frac{1}{2}, \frac{3}{2})$, can usually be observed for most cesium solids. However, if cesium is exposed to a sufficiently large local electric field gradient, the quadrupolar interactions increase and second- and higher order perturbations become important (*14, 15*). A lineshape analysis of the central transition under either static (*16–18*) or sample spinning (*19, 20*) conditions will then be required to give the quadrupole coupling constant, the EFG asymmetry parameter, and the isotropic chemical shift. Satellite transitions in these circumstances will be harder to observe because of both the broadening of the powder spectrum and the inhomogeneous excitation of the rf pulse.

A previous investigation of cesium in cation-exchanged mordenite has shown that satisfactory signal-to-noise ratios can be achieved after 10^5 scans under sample spinning (*21*). From the large quadrupolar coupling constant of the cesium observed in that study it was concluded that the zeolite framework exhibits strong electric field gradients related to the partial charge imposed on aluminum atoms. From the cesium chemical shift it was inferred that the cesium nucleus exhibited less ionic bonding than other cesium salts. Haase *et al.* have reported isotropic shift values for several cesium salts (*22*). The present work is, therefore, undertaken to use cesium NMR as a probe of structures of alkali-promoted copper catalysts by identification of distinguishable cesium sites.

EXPERIMENTAL

Catalysts were prepared by methods similar to those outlined previously (*1, 2*). Cit-

ric acid was added to aqueous solutions of cupric nitrate and alkali nitrate to yield one gram equivalent of acid per gram equivalent of copper and alkali. The resulting solution was evaporated under vacuum at room temperature to form a thick slurry. The slurry was dried overnight at 100°C. The solid obtained was then calcined at 350°C in air for 4 hr. It was observed that at approximately 200°C the catalyst precursor rapidly decomposed with the release of large amounts of heat and gas. The alkali-to-copper molar ratio of the calcined catalysts was determined by flame emission and atomic absorption spectroscopies.

All catalysts were tested in a single-pass, fixed-bed, flow microreactor system outlined previously (*1*, *2*). Feed gases were H_2 (>99.995%), Ar (>99.995%), and CO (>99.3%), which were further purified with molecular sieve 4A. Gases were metered by use of Brooks mass flow controllers.

The reaction vessel consisted of a 0.25-m, type 304 stainless-steel tube of 0.0092 m i.d. The reactor temperature was maintained by an air-fluidized sand bath. The internal reactor temperature was measured by a subminiature thermocouple moved within a stainless-steel protection sheath positioned axially in the reactor.

Reactor pressure was maintained by an air-actuated pressure control valve downstream from the reactor. The controller for the valve sensed the inlet reactor pressure. To minimize reactor pressure drop and avoid internal heat and mass transport limitations, we loaded the reactor with catalyst particles of 0.00013 to 0.00025 m in diameter (60/100 mesh).

On-line product analyses were performed by gas chromatography after 15 min on stream and then at 1-hr intervals. Samples were collected at elevated temperature and atmospheric pressure by using two gas sampling valves with 0.0005-liter sample loops. All postreactor lines and valves were heated to reaction temperature in order to avoid product condensation. Organic products were separated with a 0.00025-m-i.d., 30-m Supelco SPB-1 capillary column operated with a split ratio of approximately 80 : 1. Ar, CO, and CO_2 were separated on a Supelco S-2 carbosieve column. H_2 and H_2O concentrations were not determined. The various products were detected by use of a flame ionization detector and a thermal conductivity cell. Both columns were located in a single oven, which was ramped from 263 to 553 K at 10 K/min for maximum product separation. Data were acquired and analyzed with a Spectra-Physics 4000 lab station.

All reaction studies employed a H_2/CO/Ar synthesis gas of molar composition 2/1/0.5 at a gas hourly space velocity of 4000 hr^{-1}. Argon served as an internal standard for calculation of activity. Temperature and total pressure were maintained at 548 K and 5 MPa.

NMR on ^{65}Cu was performed at 62.65 MHz in a 5.2-T superconducting magnet. The spectrometer is similar to that described previously (*23*). The quality factor of the probe was optimized to $Q_f = 20$, which yielded the shortest pulse width plus receiver dead time for fixed transmitter power. A probe constructed with $Q_f = 20$, and with 1 kW peak-to-peak power, yielded a 3.1-μsec 90° pulse ($\omega_1 2\pi = 80$ kHz) and a probe ring-down-pulse-receiver dead time of about 3.5 μsec. ^{23}Na (58.23 MHz) in saturated NaCl aqueous solution was used to tune the rf pulses. The probe was returned to the resonance frequency of ^{65}Cu when the experiments on copper were performed. The pulse sequence used was a free induction decay with phase inversion of excitation pulse and subtraction of alternate scans to attenuate ringing artifacts.

To eliminate the copper background from the probe, silver wire was used to construct the coil. The empty probe did not yield an observable copper NMR signal after the 32,766 scans of data accumulation. The spin–lattice relaxation time was found to be a few milliseconds by observing the saturation magnetization as a function of the pulse delay after strings of 90° pulses. A

recycle rate as short as 50 msec did not saturate the initial magnetization. A recycle time of 0.1 sec was used in accumulating the copper spectra. The rf pulse flip angle was kept at about 45° (1.6 μsec) to obtain copper spectra because this produced a stronger transient signal for the central transition of quadrupolar copper. Because the spectral width increases as the pulse width decreases, the application of a shorter pulse produced spectra with less distortion. The intensity of the sharp copper metal peak, however, is reduced under this condition.

The presence of ^{23}Na in the sealed glass sample tubes interferes with the observation of ^{63}Cu resonance because of the closeness of the gyromagnetic ratio between ^{23}Na and ^{63}Cu. Thus, quantitative study of the Cu^+ spectra is difficult. The ^{65}Cu isotope that resonates about 5 MHz upfield of ^{23}Na and allows clearer observation of the Cu^+ resonance was, therefore, chosen in this study. Although the sensitivity may be reduced because of the lower natural abundance, this alternative proved feasible because of the abundance of copper spin present in the catalysts.

Cesium spectra, with ^{133}Cs resonating at 28.87 MHz, were taken in the same superconducting magnet used for ^{65}Cu NMR. Most samples were spun at the magic angle with a home-built variable temperature probe equipped with an Andrew-Beams type rotor (*24*). The spinning speed for the 5-mm-o.d. rotor was varied from 3.5 to 6 kHz to differentiate the rotational side bands.

The signals of ^{133}Cs is dried powders of Cs_2CO_3, CsCHO, $CsNO_3$, CsOH, CsCl, CsBr, and CsI were measured at ambient temperature. The inorganic samples and the catalysts were transferred to the rotor in a dry glovebox under helium gas and sealed with epoxy glue. Longitudinal relaxation times for each sample were measured approximately by progressive saturation with a string of $\pi/2$ pulses. A 4-sec repetition time, T_R, satisfied the requirement that T_R be $>5T_1$ and avoided magnetization saturation for all samples.

A 1-kW peak-to-peak pulse power was used. This gave a 3.2-μsec $\pi/2$ pulse. A quadrature receiver and a locally developed Fourier transform routine was used to receive and manipulate time domain data.

Both the copper and the cesium spectra were regularly checked with the resonance frequency of ^{65}Cu in CuCl or ^{133}Cs in aqueous CsCl solution to ensure that no folding of the spectrum occurred across the carrier frequency. A 16K (16,384 points) fast Fourier transform was performed on the 2K (2048) quadrature transient data. A dwell time of 0.2 μsec was used for all ^{65}Cu NMR to prevent the truncation of the broad components. The shift values are on the σ scale where upfield is positive and is referenced to CuCl powder or to 0.5 M $CsCl/H_2O$ solution. By convention, all spectra are presented with higher magnetic field drawn to the right.

RESULTS AND DISCUSSION

Copper NMR

The copper linewidth did not decrease under magic sample spinning as would be expected for inhomogeneously broadened spectra, perhaps because of the presence of a strong quadrupole interaction that does not scale according to a $3\cos^2\theta - 1$ spatial dependence and the presence of the coupling between conduction electrons and the copper nucleus. Therefore, all copper spectra were obtained under static conditions. Typical NMR spectra of ^{65}Cu in the catalysts are shown in Fig. 1 for samples $CuLi_{0.5}$, $CuNa_{0.5}$, $CuK_{0.5}$, $CuRb_{0.5}$, and $CuCs_{0.5}$. (The stoichiometry refers to the relative amount of alkali and copper.) A sharp component and much broader components are observed for most of the spectra. The sharp peak with linewidth of approximately 6 kHz resonates near the frequency Cu metal. This resonance is attributed to the presence of metallic Cu. The first moment of this peak is about 12.5 ppm upfield of the reference Cu powder, indicat-

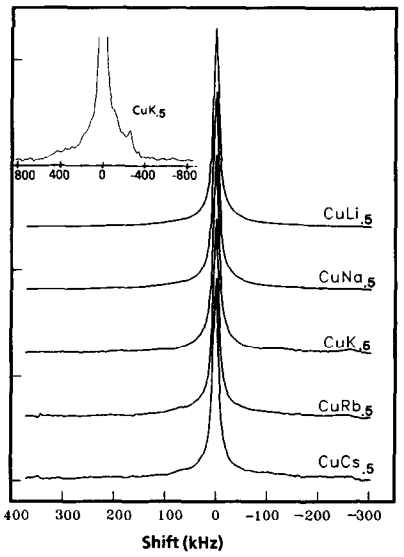

FIG. 1. ^{65}Cu NMR spectra for the alkali-promoted copper catalysts studied. The inset shows an expanded bottom portion of $CuK_{0.5}$.

ing a skin depth shift effect because the particle size is larger than the skin depth, which is estimated to be 23 μm (*9*).

Unpromoted copper prepared in the same way as the catalysts of this study shows no broad features in the NMR spectrum, indicating only metallic copper. This is consistent with the thermodynamic stability of copper in a reducing environment. The presence of the alkali promoters in the catalysts is correlated with the observed broad feature, which poses this question: Is this broad feature associated with some form of metallic copper, Cu(I), or some other oxidation state? It has been shown by comparison of metal dispersion data and NMR data for silica-supported copper that surface copper atoms in metal particles are invisible to NMR because of the magnitude of the quadrupolar broadening (*25*). Second-layer atoms appear as bulk copper. Consequently, we exclude the possibility that this broad feature is due to metallic copper in a surface or near-surface region. Previous studies of wide-line NMR of Cu in Cu_2O revealed that the quadrupole coupling constants are (e^2qQ) = 51.96 MHz and (e^2qQ) = 48.06 MHz for ^{63}Cu and ^{65}Cu, respectively (*5, 6*). Hence, the extremely wide Cu NMR spectrum that spans a range of ~400 kHz is reasonably attributed to the Cu(I) phase since other copper oxidation states are paramagnetic.

To confirm the idea that the wide-line spectra observed in the catalysts correspond to a phase containing Cu^+, the spectra of ^{65}Cu in Cu_2O and CuLiO were measured and found to be similar to the spectra of the catalysts as shown in Fig. 2. To better observe the features corresponding to Cu^+, the relatively sharp metallic Cu peak, approximated by a time domain Gaussian function, was subtracted from the total experimental time decay, and the difference decay was transformed to obtain the spectra. A Gaussian function was used because it gave the best fit to the data. The NMR

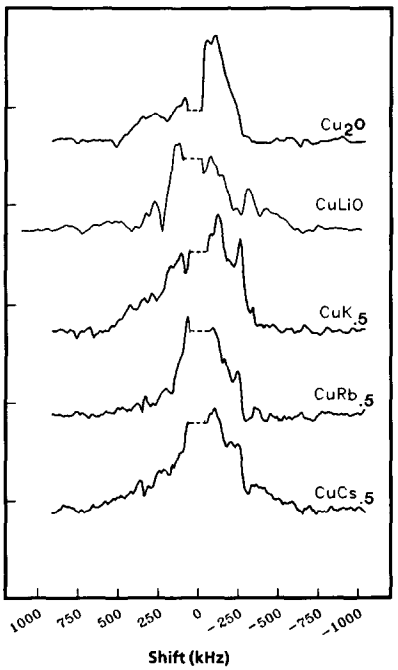

FIG. 2. The ^{65}Cu NMR spectra (62.65 MHz) for the various samples after subtraction of the Cu^0 component as fit by a Gaussian function. The spectrum of Cu_2O is shown as a comparison of the Cu^+ phase present in these samples. The lineshape shows clearly some progressive change due to different alkali promoters.

TABLE 2

Copper(I) Content and the Methanol Conversion Activity

Sample	Cu_2O	$CuLi_{0.5}$	$CuNa_{0.5}$	$CuK_{0.5}$	$CuRb_{0.5}$	$CuCs_{0.5}$
Cu(I)(%)[a]	95	3	1	13	21	17
Activity[b]		1.0	2.1	15	18	14

[a] Atomic percentage of the Cu^+ phase is obtained (assuming e^2qQ for Cu^+ in all catalysts are the same and that the Cu^{2+} phase is negligible).
[b] The steady-state activity is in $(kg/m^2/hr) \times 10^{-5}$.

spectra of Cu(I) in these samples are shown in Fig. 2. Not shown are the spectra of the Li and Na promoted samples, for which the intensities of the Cu^+ portion in the ^{65}Cu signal were relatively low. The ^{65}Cu NMR of Cu_2O and CuLiO powder are shown as a comparison. An oscillating portion of the spectra near metallic Cu resonance representing a small fraction of the signal intensity is due to the slight mismatch in the Gaussian lineshape fitting of the component associated with Cu^0 in the time domain decay and has been deleted from the results shown in Fig. 2.

The integrated area corresponding to the Cu(I) phase is larger than that of the Cu^0 phase. The sharp copper metal intensity was reduced about 40% by application of a pulse with flip angle of 45°. Therefore, the area ratio of the signals associated with these two Cu species serves only to indicate the relative trend of the amounts of the two phases in different samples but not as a quantitative measure of the mole ratios of the two phases. If we assume that all Cu^+ possess similar quadrupolar coupling constants and note that the amount of Cu^{+2} present, as determined by X-ray photoelectron spectroscopy, is negligible (*2*), the Cu^+-to-total copper ratio for the five samples may be calculated after correction for the unequal magnetizations in Cu^+ and Cu^0 associated with the $\simeq\pi/4$ flip angle in the NMR experiment. The results are tabulated in Table 2 together with the reactivity of these catalysts for comparison. The relative amounts of the Cu(I) phase correlate well with the catalytic activity of methanol synthesis (see Fig. 3).

As mentioned previously, the spin Hamiltonian governing the copper lineshape contains a quadrupole interaction and a Knight shift anisotropy of approximately the same strength. Detailed and reliable lineshape analysis that yields the interaction parameters of these interactions can in principle be achieved through a variable magnetic field study (*7*). This analysis, however, depends upon a reliable lineshape. Because of the limiting rf excitation, this is impossible to achieve for such wide-line spectra using pulse NMR without recourse to spin-echo mapping. For the present purposes, it is concluded from the copper NMR that Cu^+ is present in the catalysts and the relative concentrations of the phase(s) containing Cu^+ can be roughly estimated and found to be correlated with the catalytic activity toward syngas conversion to methanol.

NMR of Cesium

In an attempt to characterize the possible identities of the Cu(I) phase(s) believed to be the active center for the syngas conversion, the NMR of ^{133}Cs was studied in the Cs-promoted catalyst. From the extent to which the spectrum of Cs in this catalyst

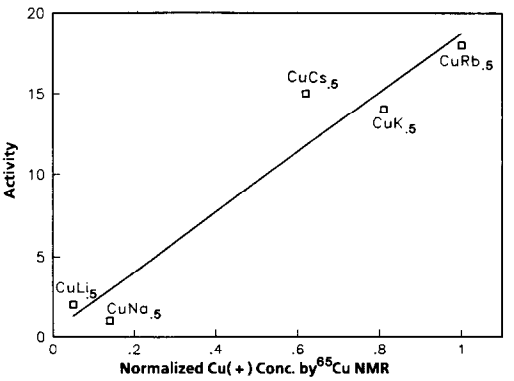

FIG. 3. The catalytic activity (in $kg/m^2/hr \times 10^5$) is shown to correlate with the Cu^+ contents ratioed to the highest Cu^+ concentration.

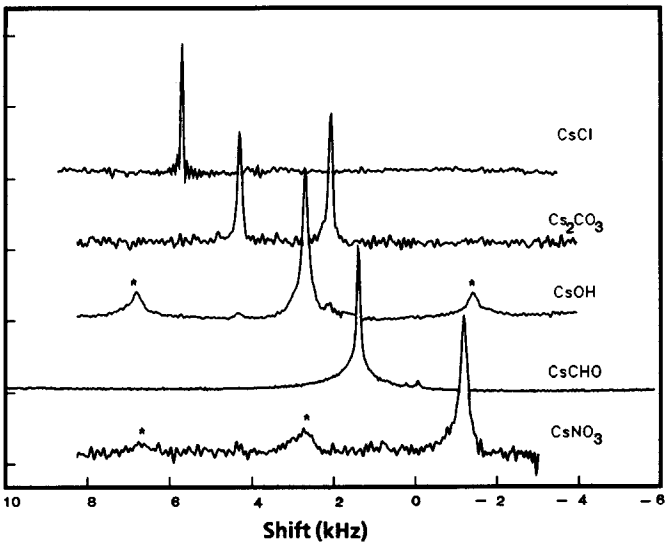

FIG. 4. ^{133}Cs MAS-NMR spectra for several selected cesium compounds. (The cesium formate spectrum is for a static sample.) The rotor frequency is 4.2 kHz. All samples were properly dehydrated and transferred to the rotor in dry box. The spinning sidebands are noted in *.

has been perturbed relative to that of ^{133}Cs in model compounds, the factors that stabilize the Cu^+ phase and the structure and the mechanism of the catalytic reaction might be inferred. The study was performed by using MAS on ^{133}Cs for the cesium-promoted catalyst.

To establish a data base from which to evaluate the cesium spectra for the catalysts a series of measurements was first performed on some stable cesium salts. Typical spectra for selected cesium salts under MAS are shown in Fig. 4. The chemical shift and the quadrupolar coupling constants for these salts are tabulated in Table 3. Simple calculations according to Samoson (*26*) and Freude *et al.* (*27*) show that the second-order quadrupole shift is no more than 1 ppm for cesium, with e^2qQ as large as 500 kHz at υ_0 = 28.78 MHz. Hence, the second-order quadrupolar shift is neglected.

A comparison of the cesium spectra of the catalysts with those of the reference cesium salts shows that the spectra of the catalysts resemble most that of the cesium carbonate, with the caveat that a third peak located somewhat downfield of Cs in CsOH is also present. The cesium spectra of the reduced catalyst and of Cs_2CO_3 are superimposed in Fig. 5. A resemblance can be seen between the ^{133}Cs NMR of the catalysts and that of Cs_2CO_3 from both the relative intensities and the two resonance frequencies. This presence of carbonate species in these catalysts has been observed by X-ray photoelectron spectroscopy of the C 1*s* peak (*2*). The linewidths, however, are broader in both resonances of the catalysts. Also, the longitudinal relaxation time of the ^{133}Cs contributing to the two outer peaks observed in the catalyst was reduced to 0.5 sec compared with a value of 2 sec observed for pure cesium carbonate. The two resonances with a 1 : 1 area ratio in Cs_2CO_3 correspond to two distinguishable cesium sites (*28*). One cesium resides near the carbonate and the other compensates for the framework charge. On the basis of the ionic character of the two cesium sites and the data on chemical shifts shown in Table 3, the cesium nucleus closer to the carbonate is assigned to the downfield peak (178.1 ppm), while the upfield peak (99.4

TABLE 3

List of Center of Mass, σ_{cm}, and the Quadrupolar Constants for a Variety of Cesium-Containing Materials

Salts	σ_{cm}(ppm)[a]	e^2qQ (kHz)
CSI	272.0	~0
CsBr	259.0	~0
CsCl	226.0	~0
Cs_2CO_3	178.1	86.0
	99.4	60.0
CsCN[b]	136.0	100.0
CsOH[c]	121.6	98.0
Cs_2SO_4	102.0	
	67.0	~260.0
CsCHO	77.2	~50.0
$CsClO_4$[b]	0.0	135.0
$CsNO_3$	−12.5	148.0
$CsCrO_4$	−64.0	75.0
Cs/mordenite[d]	−24.0(VI)	3.1 MHz
	−157.0(II)	
	−186.0(IV)	
Cs_2 molecule[e]	−130.0	
Cs free atom[e]	−350.0	

[a] Center of mass as referenced to 0.5 *M* CsCl aqueous solution was obtained by zeroing the first moment. The second-order correction was performed only for cesium-exchanged mordenite.

[b] Values from Ref. (*13*).

[c] Consistent with values from Ref. (*34*).

[d] From Ref. (*21*).

[e] From Ref. (*22*).

ppm) is assigned to be the cesium pair where bonding is relatively covalent.

The extra peak appearing between the two previously discussed resonances in the cesium spectrum of the reduced catalyst is now discussed. To investigate the nature of this peak the ^{133}Cs MAS experiments were performed under various recycle rates and different pulse flip angles. The spectra for two chosen recycle rates and flip angles are shown in Fig. 6. The intensity of the central peak relative to the two outer transitions is found to increase as the recycle times decreases. However, the relative intensity between the two outer transitions maintains a constant 1 : 1 area ratio under different recycle times. The shorter longitudinal relaxation time is associated with the central peak. From this measurement T_1 is estimated to be about 250 msec for the cesium species associated with the center peak. The cesium nuclei in the phase that at this point is identified as a carbonate-like phase in the catalyst have a T_1 of 0.5 sec, shorter than that found for pure cesium carbonate. The faster longitudinal relaxation rate than that of pure Cs_2CO_3 and the other cesium salts is taken to imply the presence of Cu within the cesium carbonate phase of the catalyst.

When the rf pulse flip angle is increased from 22.5° to 45°, the intensity of the two outer transitions decreases, indicating that the $(I + \frac{1}{2})$ rf scaling relation is satisfied for this $I = \frac{7}{2}$ nucleus. This result implies that the quadrupole coupling constant of these cesium species is larger than that in the model cesium salts measured in the present work (see Table 3). This large quadrupolar coupling constant gives rise to a broader line for ^{133}Cs in the carbonate-like phase of the catalyst than in Cs_2CO_3. In addition, there is a slight shift of the first moment due

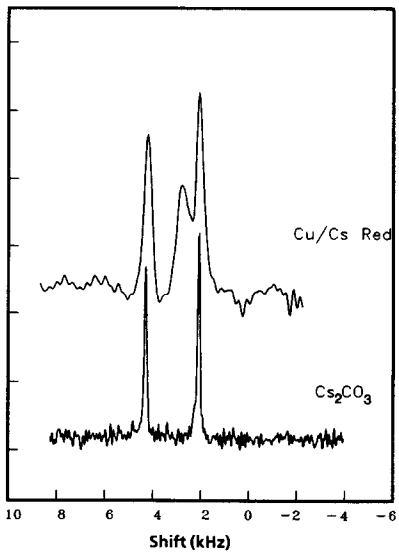

FIG. 5. Comparison of the cesium spectra of the reduced catalyst and the cesium carbonate. The appearance of the third peak in the center is due to the presence of Cu^+ phase in the catalyst which is stabilized by the cesium carbonate structure, $CsCuCO_3$. The sealed samples were spun at 4.3 kHz.

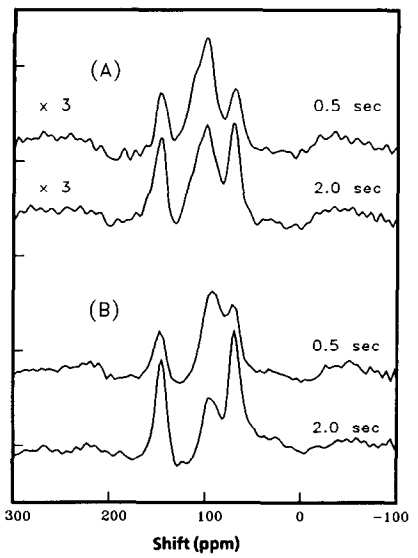

FIG. 6. The cesium spectra are shown for recycle times of 2 and 0.5 sec with rf pulse flip angles of 22.5° and 45°, respectively. Note that the two outer transitions maintain about the same 1 : 1 area ratio under all conditions. This study shows that the two outer transitions correspond to cesium carbonate, which has a T_1 of 0.5 sec, and the center peak corresponds to another cesium compound that stabilizes Cu^+ and has a T_1 of 250 msec. See text for details.

to the second-order quadrupole effects of the MAS spectra (*24, 26*). The central peak, although broader than the two outer transitions, does not follow this scaling relation, implying that the quadrupolar coupling constant for this cesium species must be smaller than that for Cs in the model compounds. The origin of the line broadening may be due to the coupling with localized, unpaired electrons or free electrons.

Structure of the Cu^+ Phase

Without an alkali promoter, the copper reduces to metallic copper. Similarly, under the conditions used for catalyst preparation and reaction, the alkali salt precursor without copper is transformed into alkali carbonate (*2*). Just as the presence of the alkali promoter gives rise to the broad peak in the copper spectra, the presence of copper in the cesium-promoted catalyst gives rise to the third peak in the cesium spectrum, suggesting an intimate relationship between copper and cesium. Clearly, the alkali stabilizes the Cu^+ via an interaction. It is reasonable to assume that this same interaction is responsible for the third peak in the cesium spectrum of the Cu/Cs catalyst.

From the NMR spectra of ^{65}Cu and ^{133}Cs in the Cs-promoted catalyst and the model compounds, we can suggest that one possibility for the copper and cesium interaction is that Cu(I) in the catalysts is in solid solution in the alkali carbonate framework with a structure similar to alkali silver carbonate (*28*) or alkali-cuprate oxides (*29–31*). In a previous study (*28*), it was found that under favorable conditions silver carbonate and alkaline carbonate mixtures react to produce several mixed carbonate salts such as $NaAgCO_3$, $KAgCO_3$, and $RbAgCO_3$. The crystal structure of potassium silver carbonate has been determined (*32*). This structure is not the same as the alkali carbonate structure. It is possible that Cu^+ in the systems studied forms a mixed carbonate structure such as $MCuCO_3$ (M = K, Rb, Cs). This mix may be structurally similar to $CsAgCO_3$, with the latter exhibiting only one cesium resonance instead of two resonances as in cesium carbonate. In this configuration, the neighboring Cu^+ nuclei reduce the charge on the cesium ion, resulting in a downfield shift compared to that of cesium carbonate. The reduced shielding from the Cu^+ compared to another cesium nucleus may also contribute to the downfield shift. The appearance of the new cesium species with a Cu^+ neighbor could give rise to a single cesium resonance with much shorter values of T_1 and T_2 than those in the cesium carbonate. The fact that the lithium-promoted copper catalyst is the least active in the syngas reaction may be related to the fact that the Cu^+ ion is much larger than Li^+ and, therefore, cannot be accommodated into the $LiCO_3$ structure.

The position of the third peak is slightly downfield of the resonance for the CsOH standard. For quadrupolar nuclei the peak

position is a function of spinning speed, which may have been different for the two samples. The relaxation time constants and the quadrupole coupling constant associated with the third peak infer that CsOH is not responsible for that resonance. Still, it is not possible to completely exclude the assignment of the third peak to CsOH strictly on the basis of the NMR data. The alkali hydroxides, however, are not thermodynamically stable relative to the carbonates (*1*) and the presence of CsOH does not explain the stabilization of Cu^+.

Finally it is noted that during the MAS experiments, the catalyst samples detune the probe. This effect becomes more severe as the spinning speed increases and reaches an equilibrium after spinning for a time. This behavior is accounted for by the presence of the metallic copper particles immersed in the copper-substituted alkali carbonate like phases in the catalysts. Metal particles with large magnetic susceptibilities are known to detune the probe when the sample is static (*33*). As the spinning speed increases, the copper particles may pack more tightly, resulting in a higher conductivity. This factor necessitated crushing the samples and repacking. After this treatment, the detuning did not recur.

CONCLUSIONS

NMR of ^{65}Cu in the unsupported alkali-promoted copper catalysts indicates the presence of a Cu^+ phase in addition to the Cu^0 metallic phase. The relative content of the Cu^+ phase for various alkali-promoted copper catalysts is found to correlate with the reactivity of the catalyst toward conversion of syngas to methanol.

NMR of ^{133}Cs indicates that the catalysts are predominantly carbonate. This conclusion is drawn from a comparison of the NMR spectra of several cesium powder salts under magic angle spinning. The promotional effect of the alkali metal is to stabilize the Cu^+ phase.

ACKNOWLEDGMENT

The authors gratefully acknowledge Carus Chemical Co. for supplying many of the cesium standard compounds used in this work.

REFERENCES

1. Sheffer, G. R., and King, T. S., submitted for publication.
2. Sheffer, G. R., and King, T. S., submitted for publication.
3. Duncan, T. M., and Dybowski, C. R., *Surf. Sci. Rep.* **1,** 157 (1987).
4. Gerstein, B. C., and Dybowski, C. R., "Transient Techniques in Nuclear Magnetic Resonance of Solids: An Introduction to the Theory and Practice." Academic Press, New York, 1985.
5. Cox, H., and Williams, D., *J. Chem. Phys.* **32,** 633 (1960).
6. Segel, S. L., and Barnes, R. G., *Phys. Rev. Lett.* **15,** 886 (1965).
7. Von Meerwall, E. D., Creel, R. B., Griffin, C. F., and Segel, S. L., *J. Chem. Phys.* **59,** 5350 (1973).
8. Slichter, C. P., "Principles of Magnetic Resonance," 2nd ed. Springer Series in Solid State Science, Springer-Verlag, Berlin, 1978.
9. Hughes, D. G., Mohanty, S., Pandey, L., and Weichman, F. L., *Canad. J. Phys.* **63,** 397 (1985).
10. Mebs, R. W., Carter, G. C., Evans, B. J., and Bennett, L. H., *Solid State Commun.* **10,** 769 (1972).
11. Creel, R. B., Griffin, C. F., and Worth, J., *Chem. Phys. Lett.* **33,** 560 (1975).
12. Fyfe, C. A., "Solid State NMR for Chemists." CFC Press, Guelph, Ontario, 1983.
13. Mooibroek, S., Wasylishen, R. E., Dickson, R., Facey, G., and Pettitt, B. A., *J. Magn. Reson.* **66,** 542 (1986).
14. Cohen, M. H., and Reif, F., *in* "Solid State Physics" (F. Seitz and D. Turnbull, Eds.), Vol. V. Academic Press, New York, 1957.
15. Maricq, M. M., and Waugh, J. S., *J. Chem. Phys.* **70,** 3300 (1978).
16. Taylor, P. C., and Bray, P. J., *J. Magn. Reson.* **2,** 305 (1970).
17. Jellison, G. E., Jr., Feller, S. A., and Bray, P. J., *J. Magn. Reson.* **27,** 121 (1977).
18. Bauger, J. F., Taylor, P. C., Oja, T., and Bray, P. J., *J. Chem. Phys.* **50,** 4914 (1969), and references therein.
19. Samoson, A., Kundla, E., and Lippmaa, E., *J. Magn. Reson.* **49,** 350 (1982); Kundla, E., Samoson, A., and Lippmaa, E., *Chem. Phys. Lett.* **15,** 229 (1981).
20. Oldfield, E., *J. Chem. Phys.* (1985); Schram, S., and Oldfield, E., *J. Amer. Chem. Soc.* **106,** 2502 (1984).
21. Chu, P. J., Gerstein, B. C., Nunan, J., and Klier, K., *J. Phys. Chem.* **91,** 3588 (1987).

22. Haase, A. R., Kerber, M. A., Kessler, D., Kronenbitter, J., Kruger, H., Lutz, O., Muller, M., and Nolle, A., *Z. Naturforsch. A* **32,** 952 (1977).
23. Cheung, T. T. P., Worthington, L. E., Murphys, P. D., and Gerstein, B. C., *J. Magn. Reson.* **41,** 158 (1980).
24. Andrew, E. R., Fiarnell, L. H., Firth, M., Gledhill, T. D., and Rokerts, I., *J. Magn. Reson.* **1,** 29 (1969).
25. King, T. S., Goretzke, W. J., and Gerstein, B. C., *J. Catal.* **107,** 583 (1987).
26. Samoson, A., *Chem. Phys. Lett.* **119,** 29 (1985).
27. Freude, D., Hass, J., Kleinowski, J., Carpenter, T. A., and Ronikier, G., *Chem. Phys. Lett.* **119,** 365 (1985). [2nd order shift]
28. Erhardt, Von H., Schweer, H., and Seidel, H., *Z. Anorg. Allg. Chem.* **462,** 185 (1980).
29. Hestermann, K., and Hoppe, R., *Z. Anorg. Allg. Chem.* **360,** 113 (1968).
30. Hoppe, R., Nestermann, K., and Schenk, F., *Z. Anorg. Allg. Chem.* **367,** 276 (1969).
31. Klassen, H., and Hoppe, R., *Z. Anorg. Allg. Chem.* **485,** 101 (1982).
32. Papin, G., Christmann, M., and Sadeghi, N., *C. R. Acad. Sci. Paris* **284,** 791 (1977).
33. Barcley, G. A., and Hoskins, B. F., *J. Chem. Soc.* 2807 (1963).
34. McCausland, M. A. H., and Mackenzie, I. S., "Nuclear Magnetic Resonance in Rare-Earth Metal" (B. R. Coles, Ed.). Monographs on Physics. Taylor and Francis, London, 1980.